



**HAL**  
open science

## Optimized ultraviolet grayscale process for high vertical resolution applied to spectral imagers

Nadine Gerges, Camille Petit-Etienne, Marie Panabière, Jumana Boussey,  
Yann Ferrec, Cécile Gourgon

### ► To cite this version:

Nadine Gerges, Camille Petit-Etienne, Marie Panabière, Jumana Boussey, Yann Ferrec, et al.. Optimized ultraviolet grayscale process for high vertical resolution applied to spectral imagers. Journal of Vacuum Science & Technology B, Nanotechnology and Microelectronics, 2021, 39 (6), pp.062602. 10.1116/6.0001273 . hal-03448269

**HAL Id: hal-03448269**

<https://hal.univ-grenoble-alpes.fr/hal-03448269v1>

Submitted on 30 Nov 2021

**HAL** is a multi-disciplinary open access archive for the deposit and dissemination of scientific research documents, whether they are published or not. The documents may come from teaching and research institutions in France or abroad, or from public or private research centers.

L'archive ouverte pluridisciplinaire **HAL**, est destinée au dépôt et à la diffusion de documents scientifiques de niveau recherche, publiés ou non, émanant des établissements d'enseignement et de recherche français ou étrangers, des laboratoires publics ou privés.

# Optimized ultra-violet grayscale process for high vertical resolution applied to spectral imagers

Running title: Optimized UV grayscale process for high vertical resolution applied to spectral imagers

Running Authors: Gerges et al.

Nadine Gerges<sup>1, 2, a)</sup>, Camille Petit-Etienne<sup>1</sup>, Marie Panabière<sup>1</sup>, Jumana Boussey<sup>1</sup>, Yann Ferrec<sup>2</sup> and Cécile Gourgon<sup>1</sup>

<sup>1</sup>Univ. Grenoble Alpes, CNRS, CEA/LETI-Minatec, Grenoble INP, LTM, 38054 Grenoble, France

<sup>2</sup>ONERA/DOTA, BP 80100, chemin de la Hunière, 91123 Palaiseau, France

a) Electronic mail: nadine.gerges@cea.fr

NanoCarb is a miniature Fourier transform imaging spectrometer dedicated to the measurement of atmospheric CO<sub>2</sub> and CH<sub>4</sub>. The key element of NanoCarb is an array of Fabry-Perot micro-interferometers having a stepcase shape. Lateral dimensions and height of each step depend on the used material, the focusing lenses and the targetted Optical Path Difference (OPD) to be measured. In this paper, we developed a grayscale lithography process for a large surface patterning with high vertical resolution. This process is combined with plasma etching to transfer the as-obtained resist patterns into the silicon substrate. This method is an efficient and quick way for the realization of such arrays into silicon. A low contrast resist (ma-P1225G) was used for a better control of the step height and we investigated the effect of two annealing processes on the contrast curve slope: the soft bake and the post exposure bake. Therefore, combining the two processes leads to a 20 nm step height resolution in resist and 50 nm in silicon.

## I. INTRODUCTION

The H2020 SCARBO (Space CARBon Observatory) is a European project led by Airbus Defense and Space, involving several partners including ONERA and IPAG <sup>1</sup>. The project aims at designing and assessing the feasibility of a constellation of small satellites at an affordable cost for the measurement of GreenHouse Gases (GHG), CO<sub>2</sub> and CH<sub>4</sub>. NanoCarb is one of the main components of the project, a Fourier transform imaging spectrometer dedicated to GHG measurement <sup>2</sup>. The NanoCarb concept is based on two main features. The first one is consisting in a very compact static imaging interferometer, whose principle is presented by Ferrec et al <sup>3</sup>: the spectro-imager is divided into two optical sub-systems, the front optics, which consists of an afocal system with a field stop, and the interferometric core which consists of a combination of an interferometer array with a micro-lens ( $\mu$ lens) array <sup>4</sup>. The interferometric plate has a stepcase shape, and as the surfaces are semi-reflective, each step behaves like a Fabry-Perot interferometer, associated to a  $\mu$ lens, which means that in front of each  $\mu$ lens, there is an interferometer with a specific thickness, and consequently a fixed Optical Path Difference (OPD). We thus obtain a set of small images on the focal plane array (FPA), each image being associated to one thickness. The second feature of NanoCarb is to measure only a partial interferogram (as shown by Gousset et al <sup>5</sup>), that is a few OPD well chosen, depending on the spectral signature of the target species. For instance, for CO<sub>2</sub> in the ShortWave InfraRed (SWIR) region, around 1.6  $\mu$ m of wavelength, this OPD is about 5.2 mm <sup>6</sup>. Therefore, the interferometric plate of imaging spectrometer on chip (ImSPOC) must have a thickness corresponding to this OPD. The lateral dimensions are given by the lateral pitch of the microlens, and for NanoCarb it is 960  $\mu$ m. The key point is that we want to have a sub-

wavelength sampling of the partial interferogram: consequently, the height of each steps of the interferometric plate has to be as small as 50 nm, if silicon substrate (refractive index  $n_{Si}=3.4$ ) is used (this choice has two benefits explained by Ferrec et al.<sup>3</sup>).

There are several methods to achieve perfectly controlled steps in the resist and transfer them into silicon. Considering binary lithography, the realization of the silicon steps requires chaining the lithography/etching steps as many times as necessary, each iteration leading to one step inside the silicon substrate. Such a sequence is not possible for a large number of steps since it is long, and a source of defects. Therefore, it is necessary to develop a faster process, enabling to realize all the steps in one single grayscale lithography and a subsequent etching process. There are various techniques of grayscale patterning, such as special optical masks <sup>7</sup>, LED-projection <sup>8</sup>, direct-write lasers <sup>9,10</sup>, and electron-beam lithography <sup>11</sup>. The latter is not effective due to long exposure times. This article describes the challenge to develop a UV grayscale lithography process combining large surface patterning with high vertical resolution. Moreover, to transfer the as-obtained resist patterns into the silicon substrate, a plasma etching process was developed to achieve 50 nm interferometer Si steps.

## II. EXPERIMENTAL

There are several methods to fabricate perfectly controlled steps in resist and transfer them into silicon from a series of lithography/etching sequences, but in case of a large number of steps, this process is time consuming and expensive. The goal is therefore to optimize a grayscale lithography process combined with a plasma etching process so that all the steps are obtained in only one lithography/etching flow (Fig. 1).

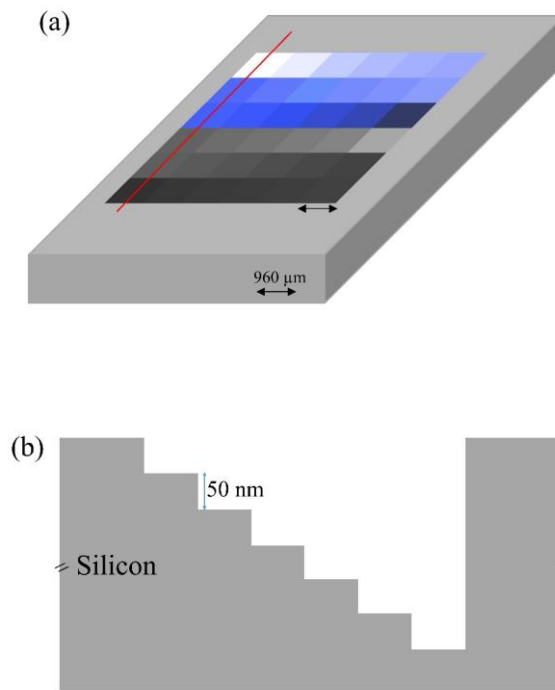


FIG. 1. (a) Illustration of a 2D micro-interferometers array of  $960 \times 960 \mu\text{m}^2$  prepared in a silicon substrate, (b): cross section along the red line showing the targeted typical step height.

### A. Lithography step

Electron beam (e-beam) grayscale lithography is well known to be able to provide the required high resolution (a few tens of nm) along the vertical direction, but is not adapted to our case, because the exposure times would be extremely long for large write-areas like  $960 \mu\text{m}$  dimension as presented above<sup>11,12</sup>. The surface size of the steps is defined by the other components of the NanoCarb device, such as the pixel dimension of the collecting camera. The conventional UV exposure is more suitable for the patterning of such large surfaces, but it is less adapted for sub-100 nm vertical resolution<sup>13</sup>. The purpose of the current work is to develop a UV grayscale lithography process combining large

surface patterning with high vertical resolution. This method comprises spatial modulation of the exposure dose, which results in a partially developed resist, and the modulation leads to the appearance of steps in the resist. Once the steps are defined in the resist, it is possible to transfer them in a single etching step into the silicon (Fig. 2).

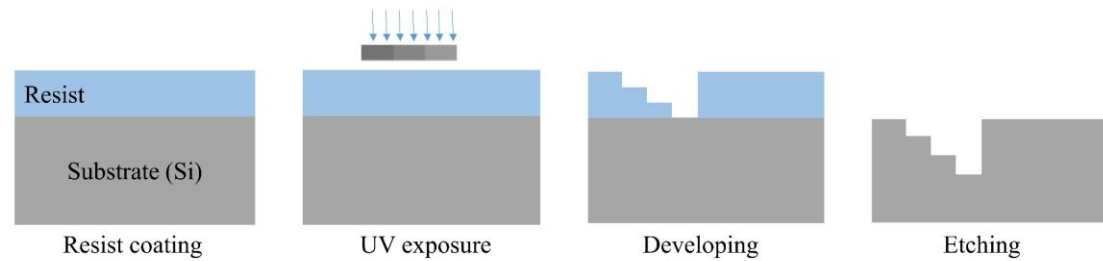


FIG. 2. Schematic representation of the realization of the steps by grayscale lithography and direct plasma etching.

We also focus on the choice of the type of the resist: a low contrast resist is necessary for grayscale lithography. Otherwise, there is no graded dependence between development rate and exposure dose. Therefore, the low contrast resist enables the thickness control in the resist after development (see Fig. 3<sup>13</sup>).

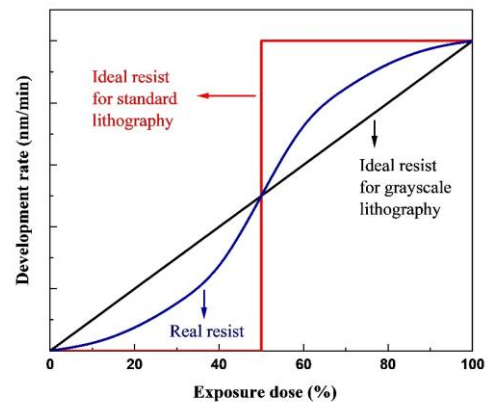


FIG. 3. Ideal characteristics of resists for grayscale or standard binary lithography.

For optical photolithography, many references report the use of the following resists: AZ5214<sup>14</sup>, SU8<sup>15</sup>, AZ4562<sup>16</sup>. AZ and SU8 resists which are basically designed for binary lithography, but their contrast can be adjusted to be compatible with grayscale lithography. Nevertheless, this contrast is still not optimal for high resolution grayscale, and therefore we used ma-P1225G positive tone resist supplied by micro resist technology GmbH that has been developed specifically for grayscale.

The 100mm-diameter silicon wafers were spin-coated with the diluted ma-P1225G at 3000 rpm for 30s to achieve a 460 nm thick film. Then the samples were baked at 100°C for 35 s in a standard process. We will show how this parameter can be optimized for our objective. In the laser lithography process, a tabletop micro pattern generator  $\mu$ PG101 (Heidelberg Instruments Mikrotechnik) was used with a modulation of beam power. In order to optimize the grayscale exposure conditions, a set of square patterns with a gradation of 10 steps was drawn using GIMP software by varying the modulation rate in the range of 0-100%. The heights of the formed photoresist structures were measured using a mechanical profilometer (DektakXT) after developing with mr-D 526/S for 15s. The height is estimated at 10% when the profilometer is properly calibrated.

Nevertheless, profilometer measurements are not always possible for such low step heights. For some samples, it was impossible to obtain a usable profile, despite visually well-defined and homogeneous steps. This is due to the fact that profilometric measurement in a polymer which is a soft material demands the use of a low force (3 mg) probe with a tip radius equal 12.5  $\mu$ m, resulting in uncertainties. Since the strips obtained have a coherent color, a new protocol based on the homogeneity of these colors is implemented with the objective of measuring the heights of the steps. The design used in

this color code is a design of three bands: two strips of 100% power exposing the entire thickness of resist are separated by an intermediate band whose height is measured by profilometer, and varies depending on the exposure power (Fig. 4). Therefore, the two side strips reach the silicon, which allows to obtain a reliable measurement of the steps. Thus, a series of power variation allows to obtain a series of colors which are directly correlated to the thickness of developed resist (Fig. 4 (c)).

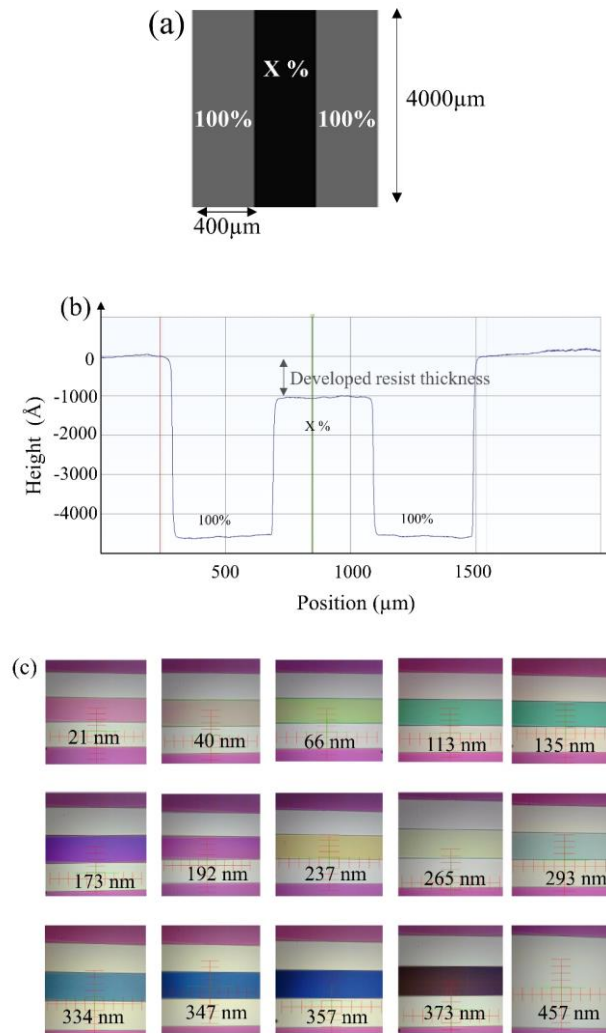


FIG. 4. (a): color code design of three strips, (b) the profile obtained in the resist, (c) heights (in nm) and optical microscopy image of strips (400\*4000 μm per strip) patterned in the resist with various power exposure ratios.

## **B. Silicon etch step**

Different approaches have been developed by many groups to transfer the resist patterns into Si. Among these groups, Kim et al.<sup>11</sup> worked on developing a grayscale technology process combining e-beam grayscale lithography with an optimized RIE process. They obtained a 1:1 ratio of the silicon to resist etching rates using SF<sub>6</sub> and O<sub>2</sub> gases. However, in their study they used a PMMA resist which is only adapted for e-beam lithography. Khazi et al.<sup>16</sup> employed also an optimized RIE process and a 1:1 ratio was achieved using SF<sub>6</sub> and CHF<sub>3</sub>. Piaszenski et al.<sup>17</sup> chose to work at a ratio 10:1 to transfer the patterns into SiO<sub>2</sub> using CHF<sub>3</sub> and O<sub>2</sub>. Nevertheless, the etching rate of these processes is usually low and we decided to use a 40 sccm Cl<sub>2</sub>, 5 sccm He/O<sub>2</sub>, 120 sccm HBr inductively coupled plasma (ICP) that was developed on an Applied Materials tool in order to transfer the as-obtained resist patterns into the silicon substrate. The interest of the process used is to be fast and very reproducible with many types of resist. The used reactor is equipped with in-situ optical characterization tools that allow a very accurate determination of the silicon etch rates. Moreover, the remaining photoresist films were stripped with an oxygen plasma in the same reactor.

## **III. Results and discussion**

Figure 5 combines two measurements; the upper one is optical microscopy image of 10 strips (400\*4000 μm per strip) patterned in the resist with various power exposure ratios and the corresponding developed resist thickness, and the lower one is the profile obtained by stripping those resist after etching the patterns into silicon.

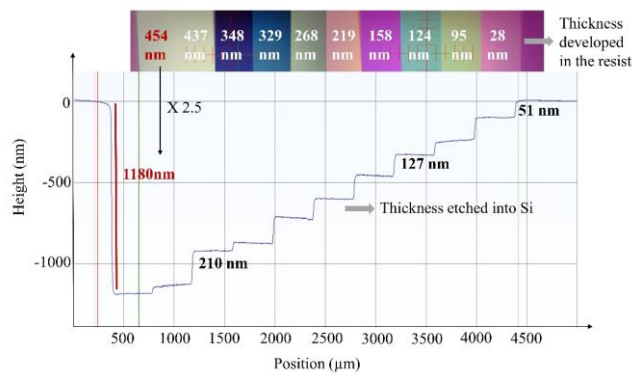


FIG. 5. Heights (in nm) and optical microscopy image of 400  $\mu\text{m}$  wide strips patterned in the resist with various power exposure ratios and the corresponding profile obtained by etching those resist patterns into silicon.

The etching time was 534 s to transfer the entire staircase into the Si. The selectivity is calculated from the thickness developed in the resist and the thickness etched in the silicon. An average selectivity value equal to 2.5 is obtained for all the stripes. The reproducibility of this ratio has been determined with tens of samples. Since the objective is to obtain 50 nm deep steps into Si, two solutions were explored: the first one was to optimize etching parameters so that the selectivity could be reduced down to 1. The second one was to use the 2.5 selectivity and to decrease the resist steps height to 20 nm.

We have therefore chosen a different etching process by replacing the He/O<sub>2</sub> (5 sccm) mixture by pure O<sub>2</sub> (10 sccm). Figure 6(a) shows the etched silicon profiles obtained for the structures after stripping resist. Unfortunately, pure O<sub>2</sub> induces micromasking on the Si surface and thus very rough profiles. A modification in power bias and pressure has been then studied with the standard (40 sccm Cl<sub>2</sub>, 5 sccm He/O<sub>2</sub>, 120 sccm HBr) mixture. We reduced the bias power from 120 W to 100 W and increased the pressure from 4 mTorr to 10 mTorr. This modification shows clearly in Fig. 6(b) that we still have a selectivity equal to 2.5. The result of Fig. 6 is representative of all the experiments and parameters

change. Nevertheless, we decided to keep the initial process thanks to its reproducibility and high etch rate<sup>18</sup> and we tried to improve the lithography process in order to increase the resolution to control 20 nm high steps in the resist.

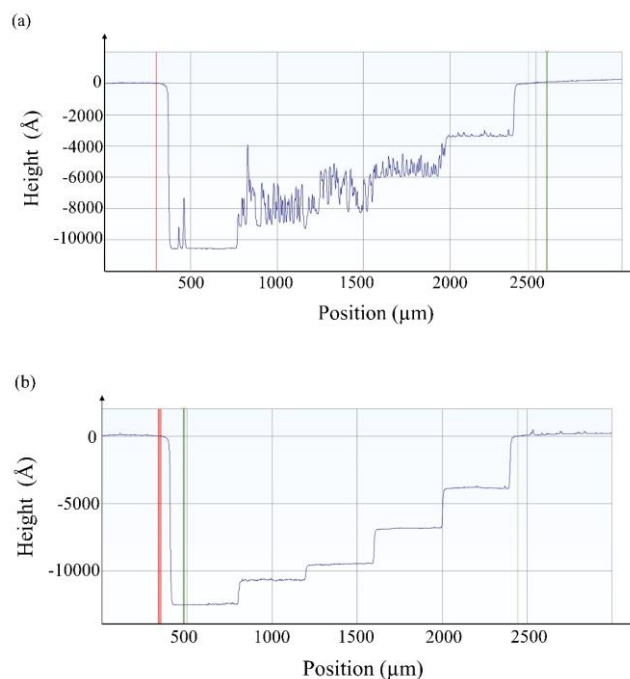


FIG. 6. The etched profiles of the stepcase shape transferred into Si (a): using  $\text{Cl}_2$ ,  $\text{O}_2$ ,  $\text{HBr}$ , (b): replacing the  $\text{O}_2$  by  $\text{He}/\text{O}_2$  with a power of 100 W bias and 10 mTorr pressure.

A better control of the step heights would be obtained with a lower contrast resist. We have demonstrated that this can be achieved by decreasing the development time, but we also explored the decrease of the contrast curve slope by studying the effect of two annealing processes: the soft bake (SB) and post exposure bake (PEB). SB allows a better evaporation of the residual solvent and a higher densification of polymer chains. We can therefore imagine that a longer annealing leads to a need for higher exposure dose, and thus to a lower developed thickness by limiting the diffusion phenomena of the chemical

reactions during the exposure. Many groups have recently studied the decrease of the slope of the contrast curves by modifying these two annealing processes. The soft bake process was optimized by Naillon et al.<sup>13</sup> for the AZ ECI 3012 resist in order to obtain a low contrast resist for grayscale lithography. They showed that this enhanced thermal treatment breaks down a significant portion of the photoactive materials, which allows to decrease the relationship between the development rate and the exposure dose. Mortelmans et al.<sup>19</sup> and Unno et al.<sup>20</sup> investigated the influence of a PEB on the dose-response behavior of PMMA and NIMO-P0701 resist, respectively, using electron beam lithography. They obtained a decrease in the depth of development if a PEB is carried out at high temperatures and for a longer time for a given dose. So in our case, we tried to investigate if such an evolution can occur in optical lithography.

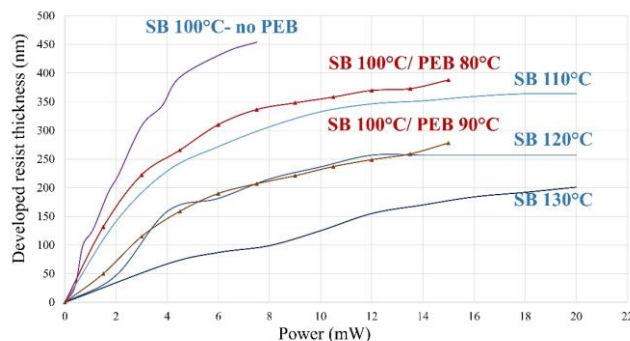


FIG. 7. Improvement of the contrast curve using various SB and PEB conditions in a 460 nm thick film of diluted ma-P1225G.

The results are presented in Fig. 7. The SB duration was 35 seconds whereas the PEB one was 5 minutes on a hotplate. As shown in Fig. 7, higher soft bake temperature decreases the resist contrast due to the densification of the resist polymer offering the lowest slope for a temperature of 130°C. This effect is what was expected and promising to increase the accuracy of our process. Generally, a PEB is used to increase the sensitivity

of the resist, and therefore decrease the necessary exposure dose. Nevertheless, in our case we observed a decrease in the contrast curve when we increased the PEB temperature (Fig.7). This result was not expected but is a benefit for the control of grayscale lithography in this resist.

We investigated the impact of PEB by Fourier-Transform-Infrared Spectroscopy (FTIR) analysis to understand what is happening in the resist during this annealing. In order to investigate the impact on the resist during the PEB annealing, we compared two situations: one with PEB (90°C – 5 minutes) and another without PEB. For both situations, the annealing analysis was carried out on a sample that was exposed and on a sample with the PEB performed just after the soft bake (100°C- 35 sec), without any exposure in order to decouple the impact of exposure and PEB (Fig.8). The CN<sub>2</sub> valence bond of the diazonaphthoquinone in the photoactive compound of the resist (2100-2200 cm<sup>-1</sup>) is clearly impacted by the exposure only. The influence of PEB is observed on the C=O bond around 1700 cm<sup>-1</sup> on Fig. 8(b). A comparison of the SB and SB-PEB cases demonstrates that heating the resist decreases this peak intensity whereas it is increased by exposure due to the formation of indene carboxylic acids. This experiment demonstrates that the PEB acts as a heating only with no correlation with exposure. If we consider the contrast curves of Fig. 7, we could expect the same peak intensity for the two cases (SB100°C-35sec/PEB90°C-5') and (SB120°C-35sec). The PEB does not induce a reaction diffusion after exposure as it occurs in many resists for deep UV lithography because they are less sensitive. Additionally, chemically amplified resists (CARs) require a PEB to induce the desired reaction. The absence of a reaction diffusion here explains why the contrast curve slope is smaller by adding a PEB in the process.

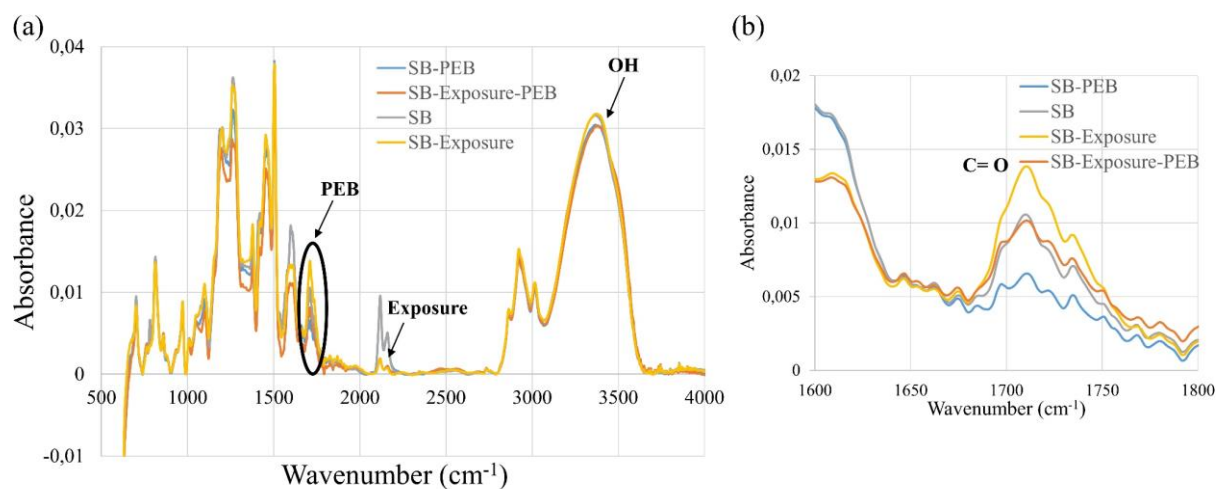


FIG. 8. (a) Results of FTIR analysis of PEB (90°C) influence, (b) a zoom after the correction. Soft Bake temperature 100°C for all samples.

This analysis helped us to optimize the process for the realization of staircase in the resist. A 130°C soft bake has been selected in order to achieve 20 nm high steps in the resist, and no PEB was applied. The exposure power for different step heights was then determined using the bottom contrast curve of Fig. 7 (SB 130°C). In Fig. 9, the profiles of resist and etched silicon obtained for the staircase are presented. As shown in this figure, the depth of the 5<sup>th</sup> and the 6<sup>th</sup> step is 118 nm and 98 nm, respectively, which results in a step height of 20 nm. This is also the case for most steps. The etching time was 455 s to transfer the entire staircase into the Si using Cl<sub>2</sub>, He/O<sub>2</sub> and HBr gases. Therefore, using these parameters we reached 20 nm in the resist and 50 nm in Si. The control of the process must be improved to accurately control all the steps. This could be attempted by using other grayscale lithography tools, for example, it would be a benefit to use an equipment with a higher control of laser beam including some integrated power control. This is the base of optimized direct laser writing new equipment because Heidelberg Instruments  $\mu$ 101 is not

the most performing and there are more advanced heidelberg laser writing systems with a software that is adapted to the correction of beam inhomogeneity. It would be interesting also to expose our patterns with a system using a digital micro-mirror device (DMD) mask. It would be therefore possible to obtain controlled a large number of 20 nm high resist steps organized in a 2D configuration by combining our process with such a tool.

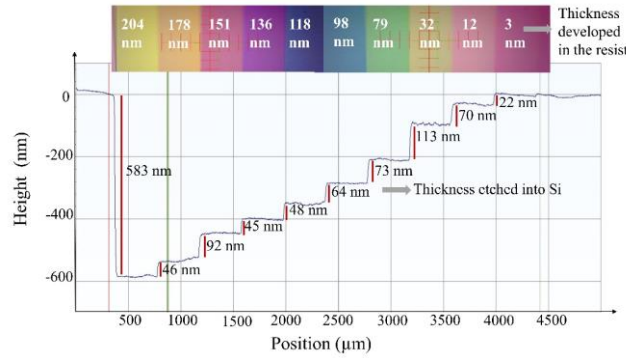


FIG. 9. Heights (in nm) and optical microscopy image of 10 strips patterned in the resist and the corresponding profile obtained by etching those resist patterns into silicon.

## IV. SUMMARY AND CONCLUSIONS

In this study, we addressed the issue of realizing a perfectly controlled staircase structure in only one lithography step and subsequent pattern transfer into silicon by plasma etching. Concerning the lithography step, we developed a UV grayscale process for a large surface patterning in a positive photoresist with very high vertical resolution. This process consists of a modulation of the exposure dose by using a micro pattern generator  $\mu$ PG101, which results in partially exposed and developed resist areas, and the modulation leads to the appearance of steps in the low contrast resist. Moreover, we developed a color code based on the homogeneity of the strips' color after exposure with the objective of measuring the heights of the steps. In order to decrease the contrast curve slope, we

investigated the impact of two annealing processes: soft bake (SB) and post exposure bake (PEB).

Furthermore, we presented a plasma etching process to transfer the as-obtained resist patterns into the silicone substrate. This process is guided by controlling the etching rates of the resist (ma-P1225G) and silicon substrate such that the desired structures are transferred into the substrates. Finally, by combining the 130°C SB annealing with an etching process with a 2.5 selectivity, 20 nm steps in the resist and 50 nm steps in silicon were fabricated, as required for the NanoCarb design. We thus enhanced the vertical height resolution of the steps by using a UV grayscale lithography process. Obtaining such a vertical resolution in silicon strips using only one grayscale lithography and plasma etching step is not only a big success for the project, but also demonstrates the capability for other lithographic applications.

## ACKNOWLEDGMENTS

This work was partially supported by the French RENATECH network and the Upstream Technological Platform (PTA).

## DATA AVAILABILITY

The data that support the findings of this study are available from the corresponding author upon reasonable request.

## REFERENCES

- <sup>1</sup> SCARBO project website, <https://Scarbo-H2020.Eu/> (n.d.).
- <sup>2</sup> S. Gousset, E. Le Coarer, N. Guérineau, L. Croizé, T. Laveille, and Y. Ferrec, in *Int. Conf. Sp. Opt. 2016* (International Society for Optics and Photonics, 2017), p. 105624U.
- <sup>3</sup> Y. Ferrec, G. Bonnery, L. Brooker, L. Croizé, S. Gousset, and E. Le Coarer, in *Int. Conf. Sp. Opt. 2018* (International Society for Optics and Photonics, 2019), p. 1118021.
- <sup>4</sup> S. Gousset, L. Croize, E. Le Coarer, Y. Ferrec, J. Rodrigo-Rodrigo, and L. Brooker, *CEAS Sp. J.* **11**, 507 (2019).
- <sup>5</sup> S. Gousset, L. Croizé, E. Le Coarer, Y. Ferrec, and L. Brooker, in *Int. Conf. Sp. Opt. 2018* (International Society for Optics and Photonics, 2019), p. 111803Q.
- <sup>6</sup> H. Ehrhardt, S. Gousset, J. Boussey, M. Panabière, E. Le Coarer, L. Croizé, Y. Ferrec, and L. Brooker, in *Int. Conf. Sp. Opt. 2018* (International Society for Optics and Photonics, 2019), p. 1118066.
- <sup>7</sup> C.M. Waits, R. Ghodssi, M.H. Ervin, and M. Dubey, in *2001 Int. Semicond. Device Res. Symp. Symp. Proc. (Cat. No. 01EX497)* (IEEE, 2001), pp. 182–185.
- <sup>8</sup> H.-C. Eckstein, M. Stumpf, P. Schleicher, S. Kleinle, A. Matthes, U.D. Zeitner, and A. Brauer, in *2015 20th Microoptics Conf.* (IEEE, 2015), pp. 1–2.
- <sup>9</sup> C. McKenna, K. Walsh, M. Crain, and J. Lake, in *2010 18th Bienn. Univ. Micro/Nano Symp.* (IEEE, 2010), pp. 1–4.
- <sup>10</sup> A. Grushina, *Adv. Opt. Technol.* **8**, 163 (2019).
- <sup>11</sup> J. Kim, D.C. Joy, and S.-Y. Lee, *Microelectron. Eng.* **84**, 2859 (2007).
- <sup>12</sup> A. Schleunitz and H. Schiff, *Microelectron. Eng.* **88**, 2736 (2011).
- <sup>13</sup> A. Naillon, H. Massadi, R. Courson, J. Bekhit, L. Seveno, P.-F. Calmon, M. Prat, and

- P. Joseph, *Microfluid. Nanofluidics* **21**, 131 (2017).
- <sup>14</sup> R.R. Benoit, D.M. Jordan, G.L. Smith, R.G. Polcawich, S.S. Bedair, and D.M. Potrepka, *IEEE Trans. Ultrason. Ferroelectr. Freq. Control* **65**, 889 (2018).
- <sup>15</sup> A. Rammohan, P.K. Dwivedi, R. Martinez-Duarte, H. Katepalli, M.J. Madou, and A. Sharma, *Sensors Actuators B Chem.* **153**, 125 (2011).
- <sup>16</sup> I. Khazi, U. Muthiah, and U. Mescheder, *Microelectron. Eng.* **193**, 34 (2018).
- <sup>17</sup> G. Piaszenski, U. Barth, A. Rudzinski, A. Rampe, A. Fuchs, M. Bender, and U. Plachetka, *Microelectron. Eng.* **84**, 945 (2007).
- <sup>18</sup> M. Panabière, C. Petite-Etienne, S. Gousset, H. Ehrhardt, and J. Boussey, in *JNTE 2019* (2019).
- <sup>19</sup> T. Mortelmans, D. Kazazis, V.A. Guzenko, C. Padeste, T. Braun, H. Stahlberg, X. Li, and Y. Ekinici, *Microelectron. Eng.* **225**, 111272 (2020).
- <sup>20</sup> N. Unno, J. Taniguchi, M. Shizuno, and K. Ishikawa, *J. Vac. Sci. Technol. B Microelectron. Nanom. Struct. Process. Meas. Phenom.* **26**, 2390 (2008).

## List of Figure captions

FIG. 1. (a) Illustration of a 2D micro-interferometers array of  $960 \times 960 \mu\text{m}^2$  prepared in a silicon substrate, (b): cross section along the red line showing the targeted typical step height.

FIG. 2. Schematic representation of the realization of the steps by grayscale lithography and direct plasma etching.

FIG. 3. Ideal characteristics of resists for grayscale or standard binary lithography.

FIG. 4. (a): color code design of three strips, (b) the profile obtained in the resist, (c) heights (in nm) and optical microscopy image of strips ( $400 \times 4000 \mu\text{m}$  per strip) patterned in the resist with various power exposure ratios.

FIG. 5. Heights (in nm) and optical microscopy image of  $400 \mu\text{m}$  wide strips patterned in the resist with various power exposure ratios and the corresponding profile obtained by etching those resist patterns into silicon.

FIG. 6. The etched profiles of the stepcase shape transferred into Si (a): using  $\text{Cl}_2$ ,  $\text{O}_2$ ,  $\text{HBr}$ , (b): replacing the  $\text{O}_2$  by  $\text{He}/\text{O}_2$  with a power of 100 Wbias and 10 mTorr pressure.

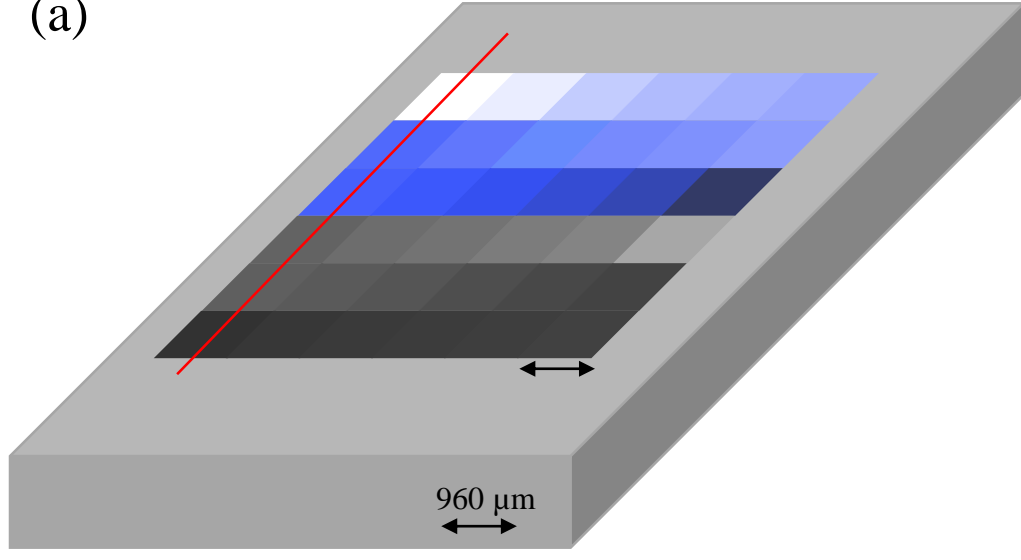
FIG. 7. Improvement of the contrast curve using various SB and PEB conditions in a 460 nm thick film of diluted ma-P1225G.

FIG. 8. (a) Results of FTIR analysis of PEB ( $90^\circ\text{C}$ ) influence, (b) a zoom after the correction. Soft Bake temperature  $100^\circ\text{C}$  for all samples.

FIG. 9. Heights (in nm) and optical microscopy image of 10 strips patterned in the resist and the corresponding profile obtained by etching those resist patterns into silicon.

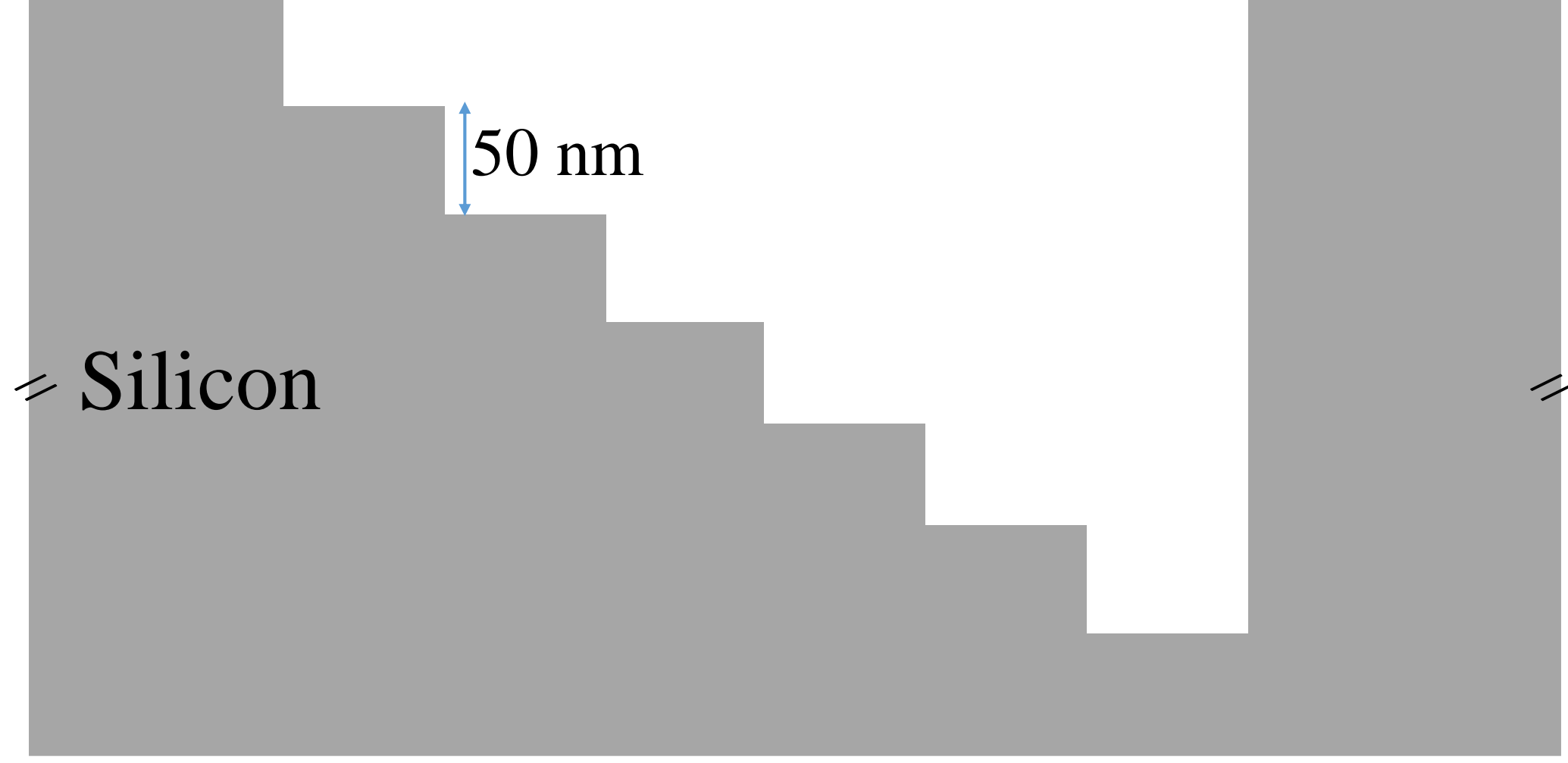
This is the author's peer reviewed, accepted manuscript. However, the online version of record will be different from this version once it has been copyedited and typeset.  
PLEASE CITE THIS ARTICLE AS DOI: 10.1116/6.0001273

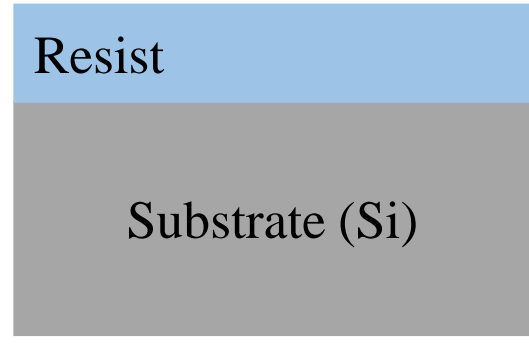
(a)



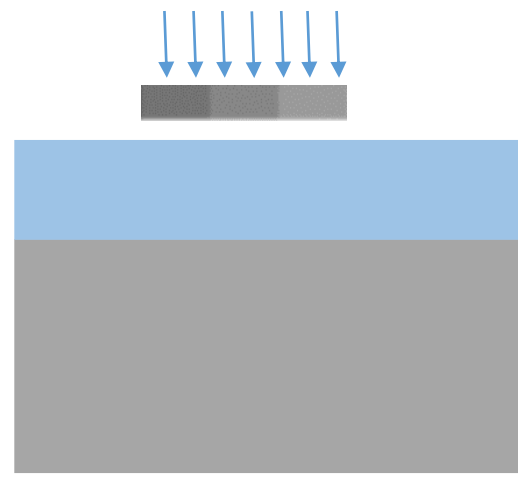
This is the author's peer reviewed, accepted manuscript. However, the online version of record will be different from this version once it has been copyedited and typeset.  
PLEASE CITE THIS ARTICLE AS DOI: 10.1116/6.0001273

(b)





Resist coating



UV exposure

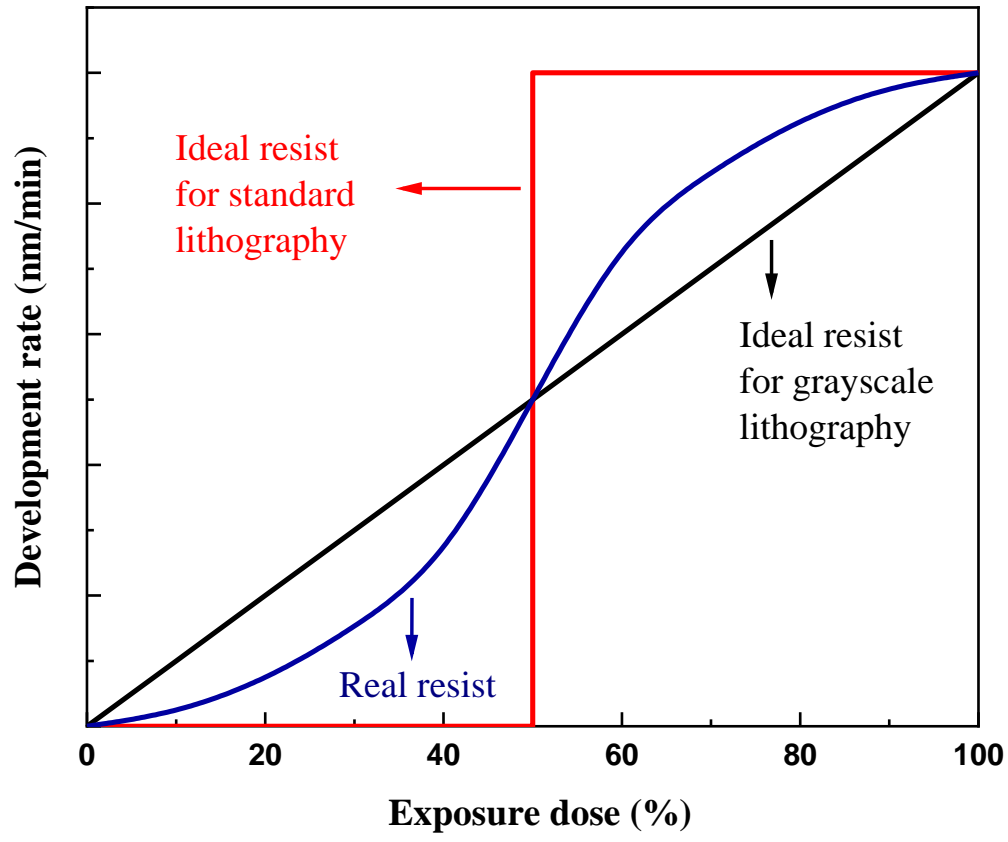


Developing

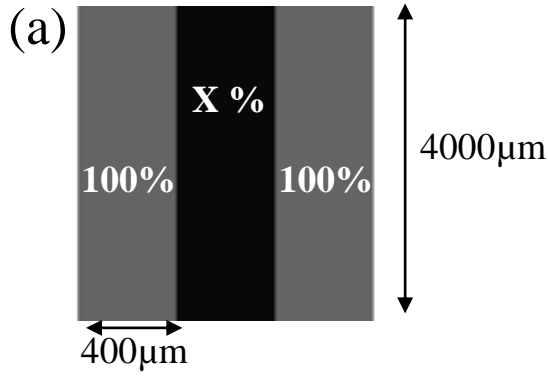


Etching

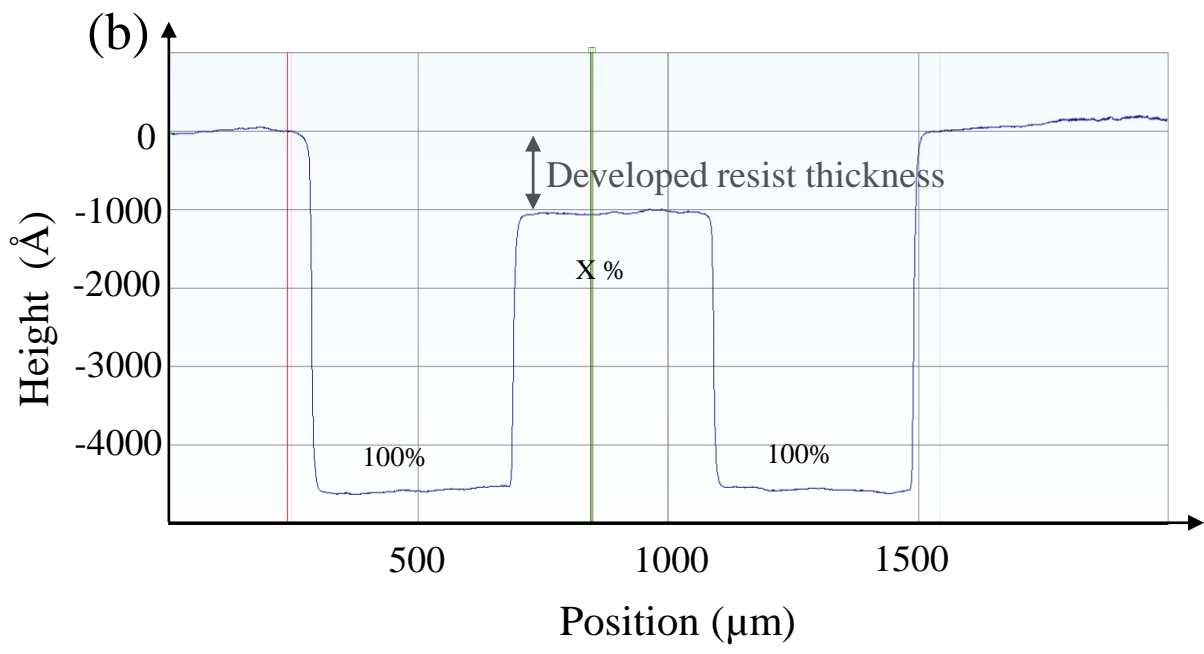
This is the author's peer reviewed, accepted manuscript. However, the online version of record will be different from this version once it has been copyedited and typeset.  
PLEASE CITE THIS ARTICLE AS DOI: 10.1116/6.0001273



This is the author's peer reviewed, accepted manuscript. However, the online version of record will be different from this version once it has been copyedited and typeset.  
PLEASE CITE THIS ARTICLE AS DOI: 10.1116/6.0001273

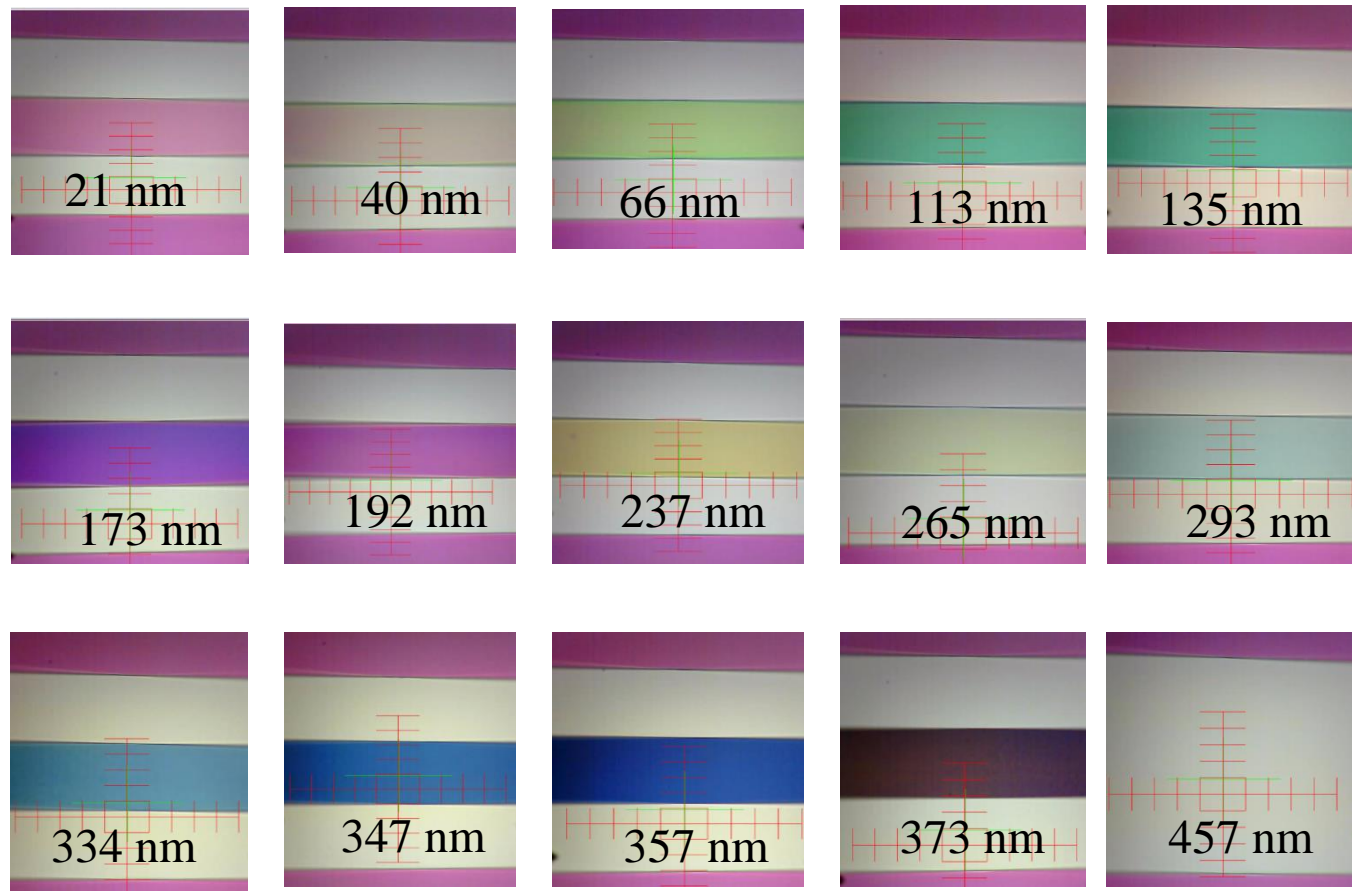


This is the author's peer reviewed, accepted manuscript. However, the online version of record will be different from this version once it has been copyedited and typeset.  
PLEASE CITE THIS ARTICLE AS DOI: 10.1116/6.0001273

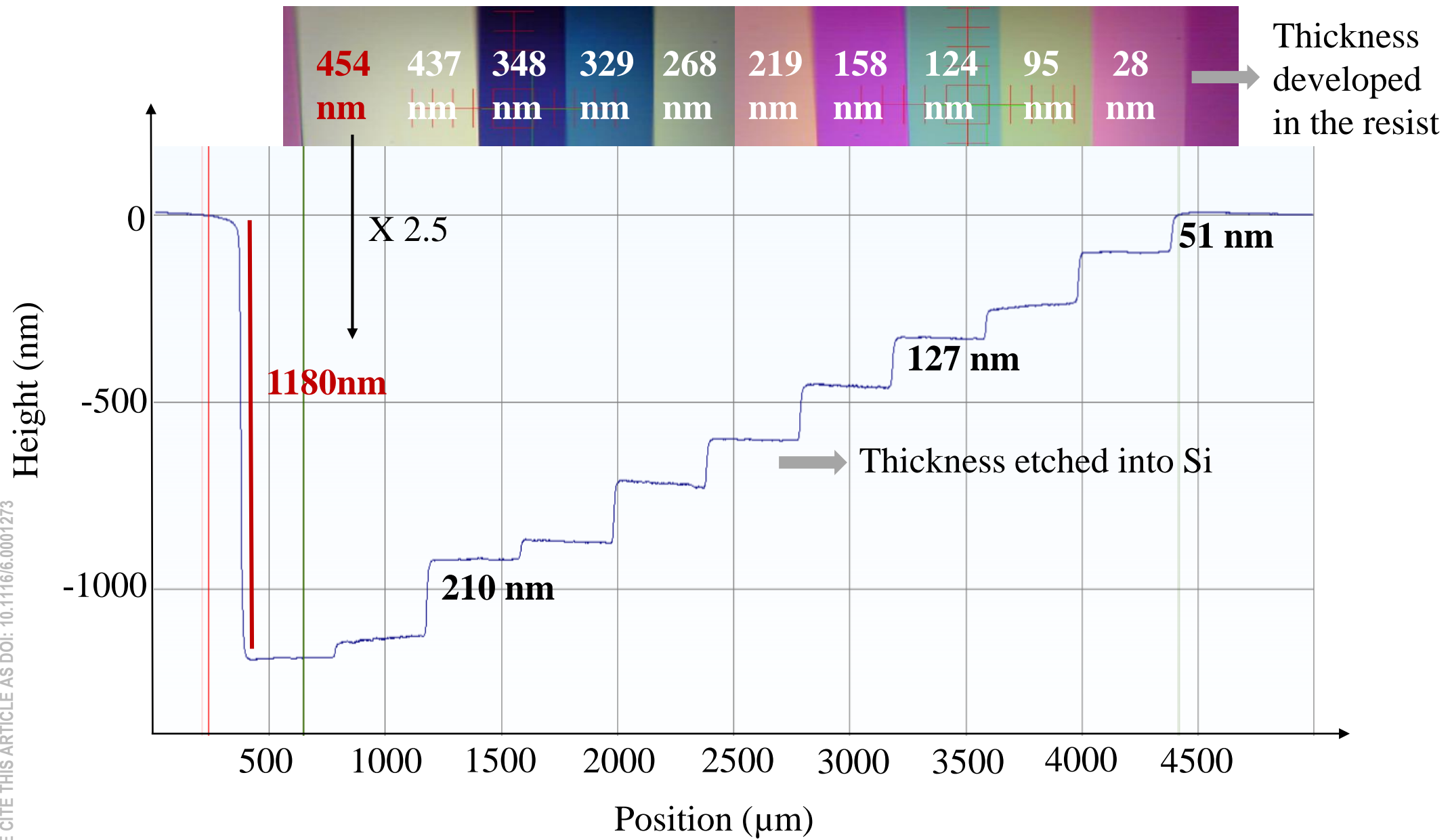


This is the author's peer reviewed, accepted manuscript. However, the online version of record will be different from this version once it has been copyedited and typeset.  
PLEASE CITE THIS ARTICLE AS DOI: 10.1116/6.0001273

(c)

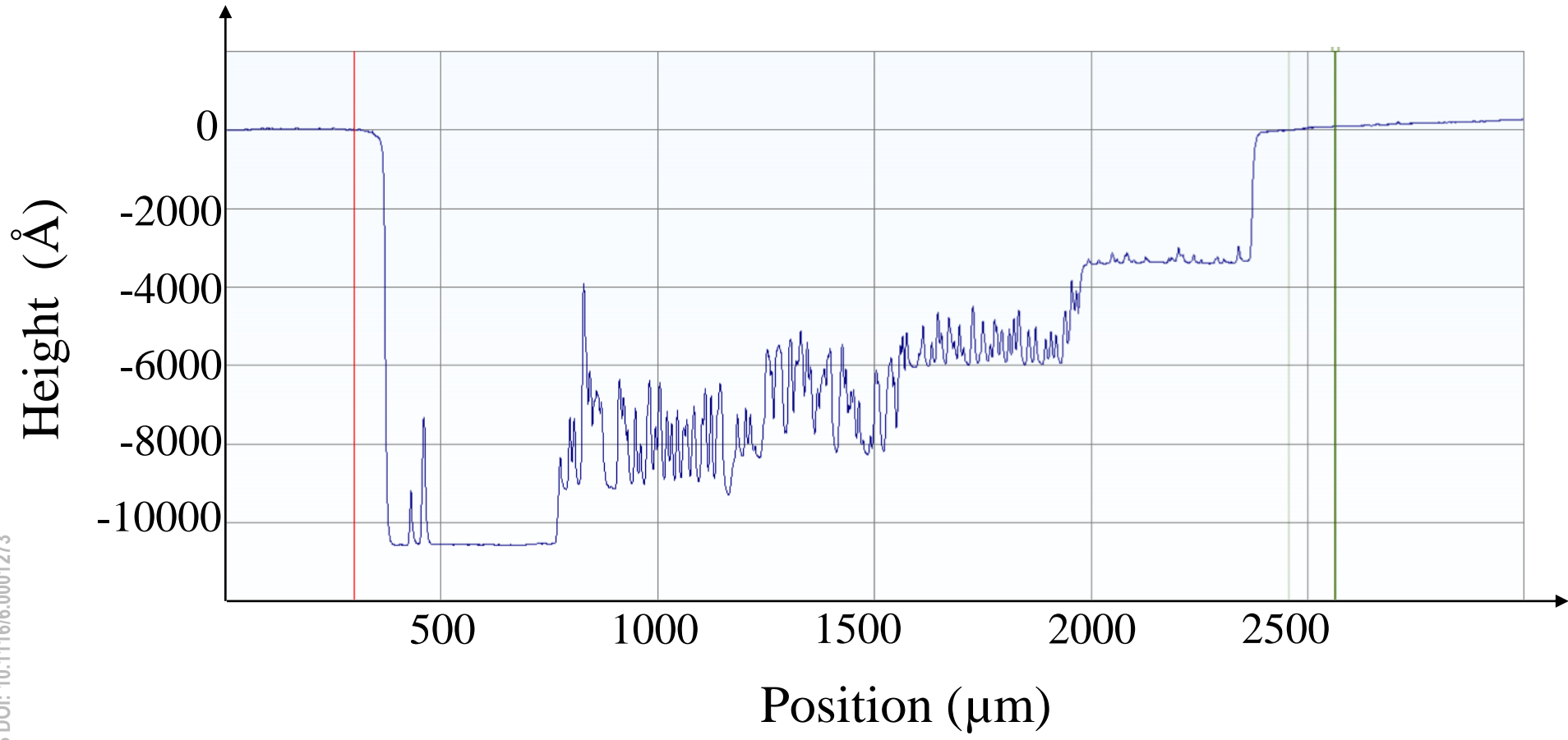


This is the author's peer reviewed, accepted manuscript. However, the online version of record will be different from this version once it has been copyedited and typeset.  
PLEASE CITE THIS ARTICLE AS DOI: 10.1116/6.0001273



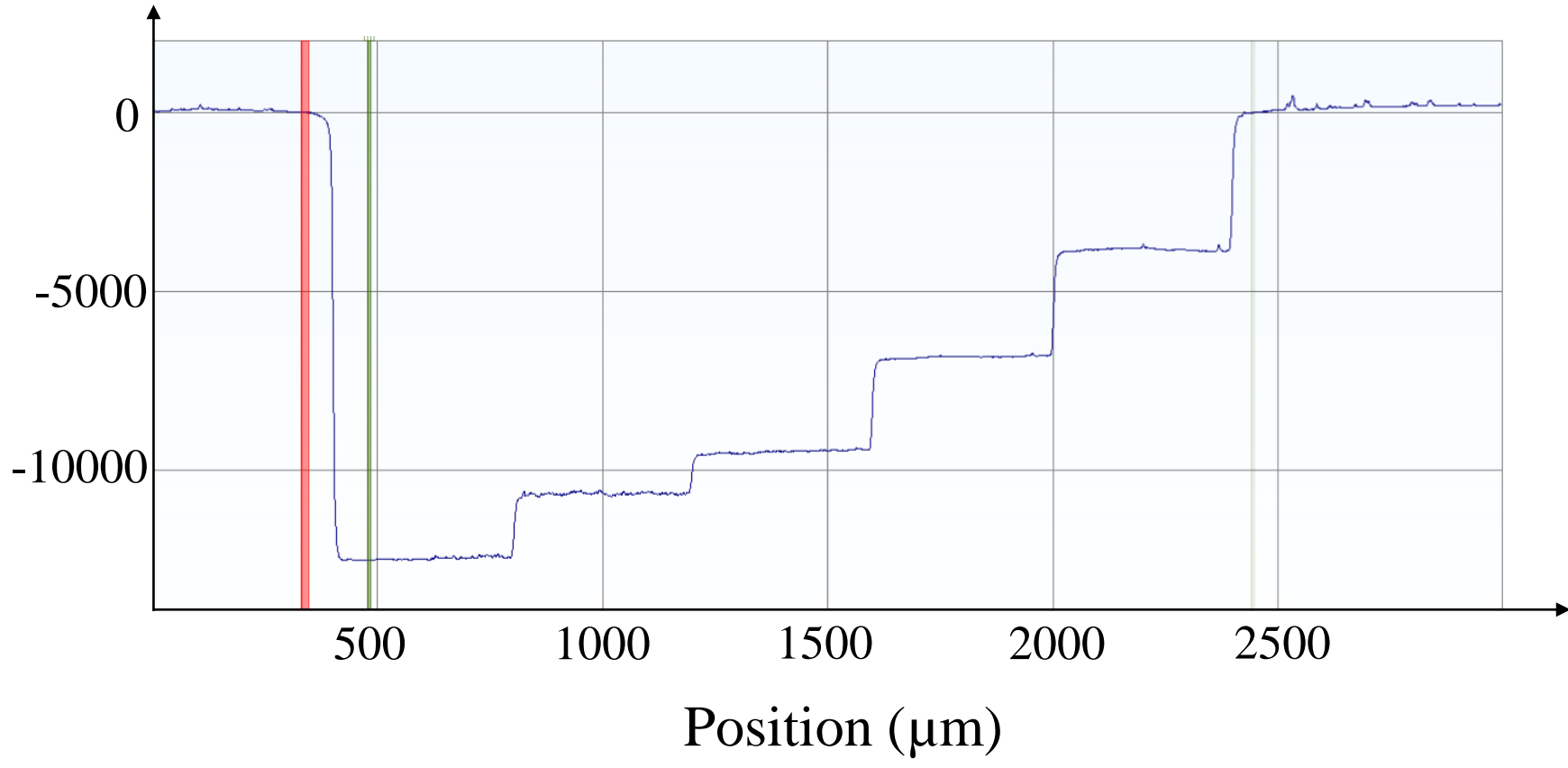
This is the author's peer reviewed, accepted manuscript. However, the online version of record will be different from this version once it has been copyedited and typeset.  
PLEASE CITE THIS ARTICLE AS DOI: 10.1116/6.0001273

(a)



This is the author's peer reviewed, accepted manuscript. However, the online version of record will be different from this version once it has been copyedited and typeset.  
PLEASE CITE THIS ARTICLE AS DOI: 10.1116/6.0001273

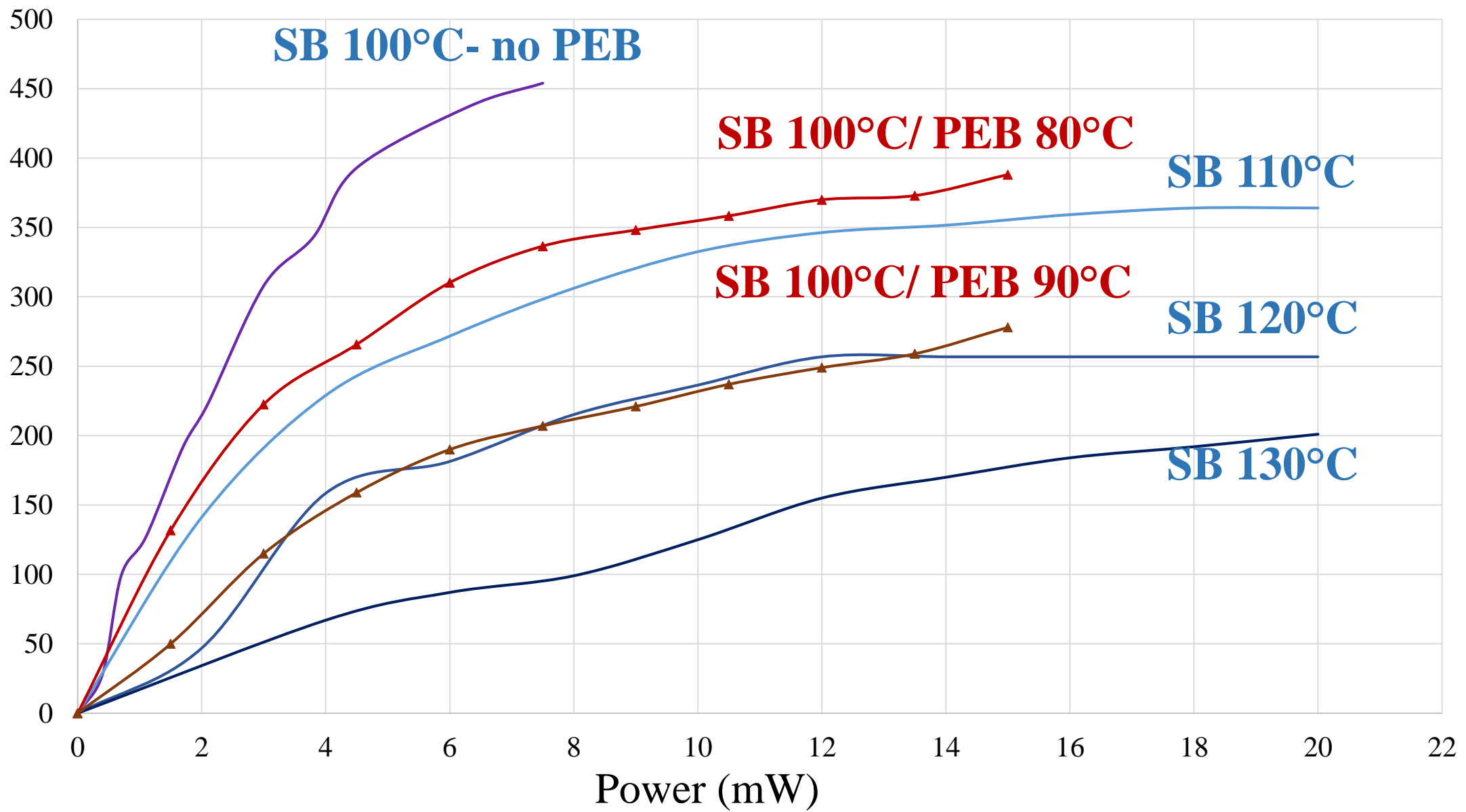
(b)  
Height (Å)



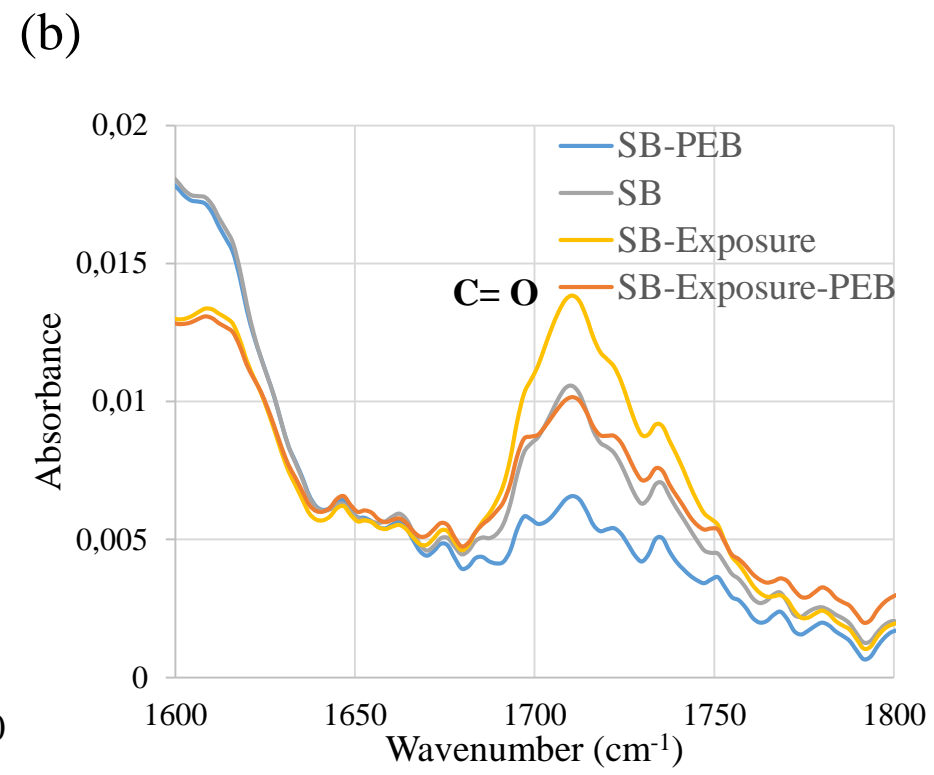
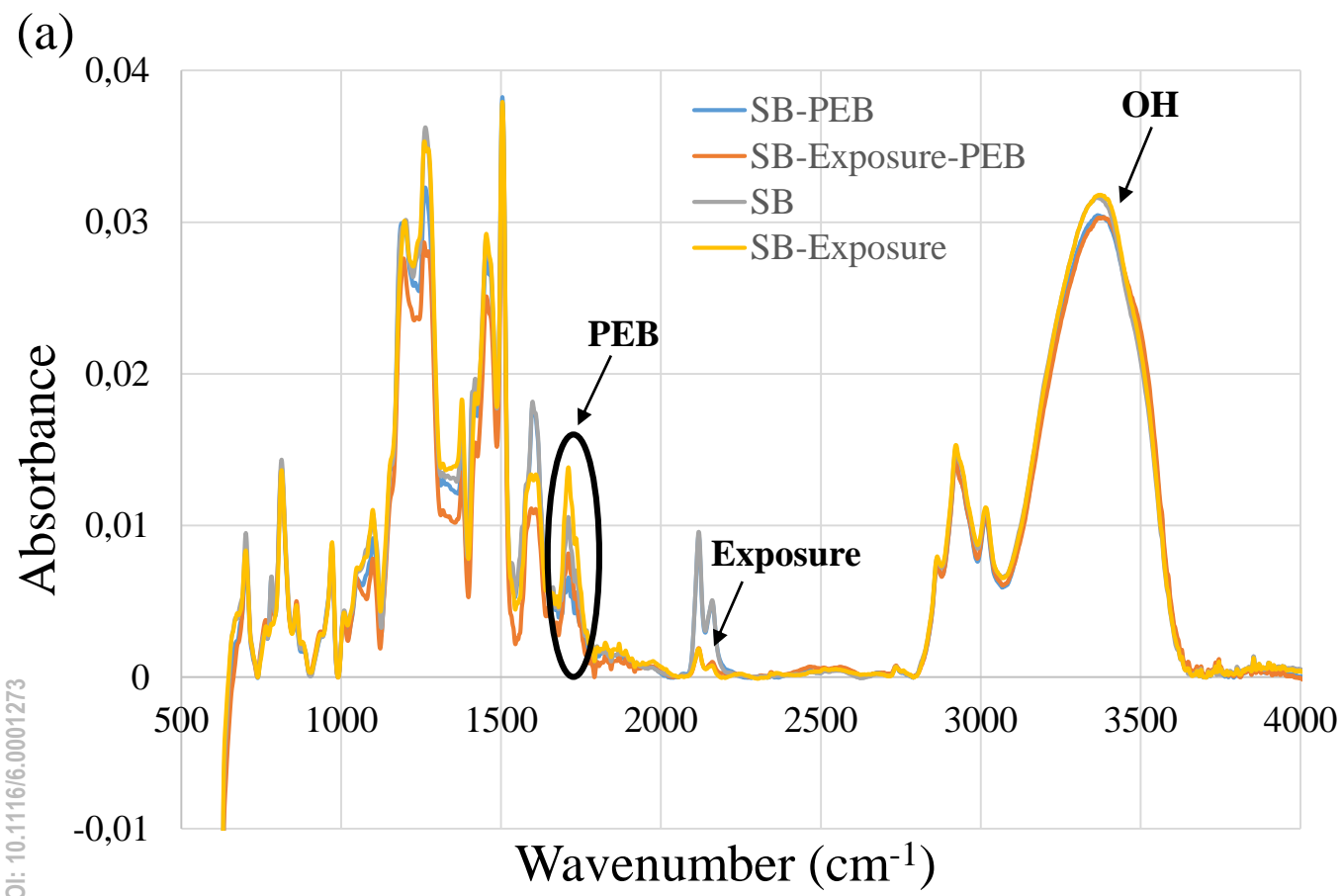
This is the author's peer reviewed, accepted manuscript. However, the online version of record will be different from this version once it has been copyedited and typeset.

PLEASE CITE THIS ARTICLE AS DOI: 10.1116/1.5001173

Developed resist thickness (nm)



This is the author's peer reviewed, accepted manuscript. However, the online version of record will be different from this version once it has been copyedited and typeset.  
PLEASE CITE THIS ARTICLE AS DOI: 10.1116/6.0001273



This is the author's peer reviewed, accepted manuscript. However, the online version of record will be different from this version once it has been copyedited and typeset.  
PLEASE CITE THIS ARTICLE AS DOI: 10.1116/6.0001272

